

A Model for Monomer and Micellar Concentrations in Surfactant Solutions. Application to Conductivity, NMR, Diffusion and Surface Tension data.

Wajih Al-Soufi^{}, Lucas Piñeiro, and Mercedes Novo*

Department of Physical Chemistry, Faculty of Science, University of Santiago de Compostela, E-27002 Lugo, Spain.

Corresponding author: e-mail: wajih.al-soufi@usc.es . Tel.: + (34) 982824114 Fax: + (34) 982824001

Abstract: An empirical model for the concentrations of monomeric and micellized surfactants in solution is presented as a consistent approach for the quantitative analysis of data obtained with different experimental techniques from surfactant solutions. The concentration model provides an objective definition of the critical micelle concentration (*cmc*) and yields precise and well defined values of derived physical parameters. The use of a general concentration model eliminates subjective graphical procedures, reduces methodological differences, and thus allows one to compare directly the results of different techniques or to perform global fits. The application and validity of the model is demonstrated with electrical conductivity, surface tension, NMR chemical shift and self-diffusion coefficient data for the surfactants SDS, CTAB, DTAB, and LAS. In all cases the derived models yield excellent fits of the data. It is also shown that there is no need to assume the existence of different pre-micellar species in order to explain the chemical shifts and self-diffusion coefficients of SDS as claimed recently by some authors.

Keywords: Surfactants, Micelles, Critical Micelle Concentration, Concentration Model, Data Analysis

Introduction

Because of their unique solution properties surfactants are an essential component of many industrial, pharmaceutical, and environmental applications [1, 2].

Although surfactant self-aggregation has been extensively treated theoretically [3-9], none of the elaborate thermodynamic models nor the increasingly complex numeric simulations has provided so far a manageable quantitative description of the micellization process which could be used for the analysis of experimental surfactant data.

The quantitative description of the properties of surfactant solutions, such as conductivity, NMR-shift, surface tension, translational diffusion, light scattering or solute partition constants, requires knowledge of the concentrations of monomeric $[S_1]$ and micellized $[S_m]$ surfactants in solution, which in turn depend mainly on the critical micelle concentration (*cmc*) of the surfactant system.

For the analysis of experimental data it is often assumed that the no micelles are formed below the *cmc* and that above it all additional surfactant forms micelles. With the total surfactant concentration $[S]_0$, the concentrations of monomeric $[S_1]$ and micellized $[S_m]$ surfactants in solution are then obtained by the following approximation: [10, 11]

$$\begin{aligned} [S]_0 < cmc : [S_1] &\approx [S]_0, [S_m] \approx 0 \\ [S]_0 &\geq cmc : [S_1] \approx cmc, [S_m] \approx [S]_0 - cmc \end{aligned} \quad (1)$$

This simplification, although widely used, presents several problems: it introduces a discontinuity in the concentrations at the *cmc* and requires that the value of the *cmc* is determined separately. It is further generally accepted that the *cmc* has no strict meaning and that the transition from monomeric to micellized surfactant does not occur at a sharply defined concentration but within a concentration interval around the *cmc* [12].

It would be therefore desirable to have a continuous and well defined mathematical model of the concentrations of the surfactant species in solution which includes a definition of the *cmc* itself.

The characteristic concentration taken as *cmc* can be defined in different ways. A plot of the monomer

concentration $[S_1]$ or a physical property, $\phi = a[S_1] + b[S_m]$, which depends linearly on $[S_1]$ and $[S_m]$, versus $[S]_0$ typically yields two straight lines with a more or less abrupt change in their slope at the onset of the aggregation of free surfactant monomers to micelles. The *cmc* can be defined as the concentration at the point of intersection of the two straight lines [13]. However, the choice of the two linear intervals which define the straight lines is subjective and, in cases of very small changes in the slopes or of wide transition region between them, this definition can be practically inoperable. Furthermore, strong methodological differences in the determination of the *cmc* can be found, depending on the type of experiment, the way the data are processed, and how they are plotted and then analyzed [13, 14].

A generally accepted criterion for the *cmc* was given by Phillips [15], who defined the *cmc* as the concentration that corresponds to the maximum change in the gradient of a plot of the magnitude ϕ against $[S]_0$, given by a zero third derivative of ϕ :

$$\phi'''(cmc) = \left(\frac{d^3\phi}{d[S]_0^3} \right)_{[S]_0=cmc} = 0 \quad (2)$$

This “Phillips-condition” is the basis of more objective methods for the determination of the *cmc*, mostly developed for electrical conductivity data of ionic surfactants [16-19].

Based on the phase separation model [20, 21], and probabilistic arguments García-Mateos et al. [16] propose that the second derivative of ϕ with respect to $[S]_0$ (the curvature of ϕ) is well described by a Gauss function (eq (3)) centered at the *cmc*, with amplitude H and a width σ of the transition region around the *cmc*.

$$\phi'' = \frac{d^2\phi}{d[S]_0^2} = -H \cdot e^{-\frac{([S]_0 - cmc)^2}{2\sigma^2}} \quad (3)$$

The determination of the *cmc* from conductivity measurements is based on the consecutive double numerical integration of ϕ'' of eq (3) by the Euler method combined with a least squares iterative grid search for the best fitting parameters (*cmc*, σ , and H) [16]. This method is based on the phase separation model, which best describes pure micellar systems having high aggregation numbers. Nevertheless, the

authors applied it successfully to conductivity data of binary mixtures of ionic surfactants [16] and to micelles with low aggregation numbers [22]. This method has been modified by Pérez-Rodríguez et al. [18] using the Runge-Kutta method for the numerical integration of the Gaussian function and the Levenberg-Marquardt algorithm for the least squares fitting. Both methods describe specifically conductivity data and special programming effort is required for their application to experimental data.

Carnero Ruiz et al. presented a model for the conductivity κ of ionic surfactants as a function of total surfactant concentration $[S]_0$ based on the observation that the first derivative of the conductivity data can be adequately described by a Boltzmann type sigmoidal function [19]. By analytical integration of this sigmoidal function they obtain a function for the dependence of the conductivity κ on $[S]_0$. Although this model has some similarities to the one presented here, it was derived specifically for conductivity data and has different mathematical properties.

A model-free nonparametric approach to estimate *cmc* values based on local polynomial regression has been proposed by López Fontán et al. [23] It determines *cmc* values from plots of properties with an abrupt change in the slope at the *cmc* such as conductivity or osmotic coefficients and allows for an exploratory data analysis without the rigidity of parametric models. However, the complex algorithm requires a specific software-tool and the results seem to depend slightly on the chosen parameters of the regression (bandwidth). Being nonparametric it does not yield physical parameters other than the *cmc* itself.

Shanks and Franses presented conductivity models which are based on mass action micellization thermodynamics and on the Debye-Hückel-Onsager theory. Their detailed model requires numeric integration combined with a maximum likelihood method in order to obtain the best fit parameters [17]. Jalšenjak and Težak propose a model for the first derivative of conductivity versus total surfactant concentration derived from the mass action model and different conductivity models [24]. Both models are specific to conductivity data.

Starting from these definitions of the *cmc* it is now our task to find a compact analytical model of

surfactant concentrations and derived properties which is suitable for the routine analysis of experimental data from surfactant solutions without the need for further treatment or specialized algorithms. We limit this empirical model to surfactant concentrations not too far away from the *cmc* and we will concentrate here on the derivation and discussion of the concentration model and its application to physical properties which are direct functions of monomer and micellar concentrations, such as conductivity, surface tension, NMR and diffusion coefficient. In a forthcoming contribution we will deal with experiments involving additional solutes, such as fluorescent dyes, which require a more detailed analysis of the partition of the solute between the aqueous phase and the micellar pseudophase and its distribution among the micelles. The empirical concentration model does not pretend to compete with elaborate thermodynamic theories or simulations of surfactant self-assembly but to improve the empirical methods used so far.

Material and methods

Materials. Sodium dodecylsulfate (SDS), Dodecyltrimethylammonium bromide (DTAB) and Hexadecyltrimethylammonium bromide (CTAB) of purity higher than 99% were purchased from Sigma-Aldrich and used as received. Linear alkylbenzene sulfonic acid (LAB) was kindly supplied by Henkel AG (Düsseldorf, Germany) with a purity of 96%. This surfactant, commonly used in the laundry industry, is a complex mixture of homologues and isomers with a mean chain length of 11.6. To avoid pH changes, the corresponding sodium salt (Linear alkylbenzene sulfonate, LAS) was obtained by neutralization of the LAB solutions with NaOH (Sigma-Aldrich). NaH_2PO_4 and Na_2HPO_4 from Fluka were used to prepare a phosphate solution of ionic strength 0.01 M.

Conductivity Measurements.

An electrical conductivity meter Basic 30 from Crison Instruments (Barcelona, Spain) provided with a standard conductivity cell and temperature sensor Pt 1000 was used to measure the conductivity of surfactant solutions of different concentrations. The measuring solutions were prepared by dilution of stock solutions of the surfactants using two methods: (i) step-by-step dilution-extraction method [25]

starting with the surfactant stock solution (titrations with less data points as for DTAB and CTAB); (ii) addition with a burette of small volumes of the surfactant stock solution to a precise, much larger volume of water, which allows to measure a high number of data points (titrations of SDS and LAS). In both cases the temperature of the measuring solutions was controlled by circulating water through a jacketed beaker thermostated with a VWR Cryostat model 1166D with a precision of $\pm 0.05\text{K}$.

Data Analysis. All data were analyzed with OriginPro 8.5 (OriginLab Corporation, US). All given uncertainties correspond to one standard deviation from the fits and do not include calibration errors. The Origin functions of the concentration model and all derived magnitudes used are given ready to use in the supplementary data.

Theory

Empirical Model for the Surfactant Concentrations

In a strongly simplified picture, below the *cmc* all surfactant molecules are monomeric, whereas above it all additional surfactant molecules self-assemble and form micelles with a mean size given by the aggregation number n with a relatively narrow size distribution [1, 3, 26, 27]. As a result, the concentration of monomeric surfactant $[S_1]$ is equal to the total surfactant concentration $[S]_0$ below the *cmc* and stabilizes then at the value of the *cmc* itself:

$$[S_1] = \begin{cases} [S]_0, & [S]_0 \ll cmc \\ cmc, & [S]_0 \gg cmc \end{cases} \quad (4)$$

The concentration of aggregated (micellized) surfactants, $[S_m]$, is the difference between the total concentration and that of monomeric surfactants:

$$[S_m] = [S]_0 - [S_1] \quad (5)$$

The concentration of micelles, $[M]$, depends on the mean aggregation number, n , which can itself depend on the surfactant concentration $[S]_0$ (see below):

$$[M] = [S_m] / n \quad (6)$$

Our starting point are the empirical descriptions of Phillips (eq (2)) and Garcia-Mateos (eq (3)). In

contrast to other authors [16, 18] we apply eqs (2) and (3) directly to the monomer concentration $\phi = [S_1]$ (and not to conductivity) and integrate $[S_1]''$ in the following analytically, eliminating the need for numerical integrations during the application of the model. Then the second derivative of $[S_1]$ is described by a Gauss function centered at the *cmc* and with width σ as given in eq (7).

$$[S_1]'' = \frac{d^2[S_1]}{d[S]_0^2} = -A \frac{1}{\sqrt{2\pi}\sigma} e^{-\frac{([S]_0 - cmc)^2}{2\sigma^2}} = -\frac{A}{cmc} \frac{1}{\sqrt{2\pi}r} e^{-\frac{(s_0 - 1)^2}{2r^2}} \quad (7)$$

The amplitude $A > 0$ is determined later as a normalization constant. The width σ of the Gaussian is a measure of the concentration range of the transition region. The smaller σ is, the sharper is the transition between the two linear regions below and above the *cmc*. In order to facilitate the comparison of widths σ of surfactants with different *cmc* values, we define the *relative transition width* r as given in eq (8).¹

$$r = \sigma / cmc \quad (8)$$

Only to simplify the expressions, we also define a *relative total surfactant concentration* s_0 as ratio between $[S]_0$ and the *cmc*:

$$s_0 = [S]_0 / cmc \quad (9)$$

Integration of $[S_1]''$ in eq (7) gives the slope $[S_1]'$:

$$[S_1]' = \int [S_1]'' d[S]_0 = -\frac{A}{2} \operatorname{erf}\left(\frac{s_0 - 1}{\sqrt{2}r}\right) + C_1 = \frac{A}{2} \left(1 - \operatorname{erf}\left(\frac{s_0 - 1}{\sqrt{2}r}\right)\right) \quad (10)$$

The error function $\operatorname{erf}(x)$ is a sigmoid type function centered at $x=0$ (in this case at the *cmc* where $s_0=1$) with limiting values: $\operatorname{erf}(0) = 0$, $\operatorname{erf}(-\infty) = -1$, and $\operatorname{erf}(\infty) = 1$.

¹ The “transition width” σ (and $r = \sigma / cmc$) is the width of the Gaussian used to describe the second derivative $[S_1]''$ around the *cmc*. The width σ is proportional to the mathematical “radius of curvature” [62] R of $[S_1]$, $R([S_1]) = (1 + [S_1]'^2)^{3/2} / [S_1]''$, ($R(cmc) \approx 3.50 \cdot \sigma$), and is inversely proportional to the curvature $K = 1/R$ and to the second derivative at the *cmc*: $[S_1]''(cmc) \approx -(2\pi)^{-1/2} \sigma^{-1}$. It is interesting that, because $K([S_1])$ depends on both, $[S_1]''$ and $[S_1]'$, the maximum of the mathematical curvature K is found at a slightly higher concentration than the *cmc*, which is defined by the maximum of $[S_1]''$ alone according to the Phillips condition (eq (2)), $[S_1](K) \approx cmc + 0.36 \cdot \sigma$.

The integration constant C_1 in eq (10) is determined by the condition that at high surfactant concentration the monomer concentration is constant ($[S_1] = cmc$) so that its slope $[S_1]'$ approaches zero:

$$\lim_{s_0 \rightarrow \infty} [S_1]' = 0 \Rightarrow C_1 = \frac{A}{2} \quad (11)$$

A second integration already gives the concentration $[S_1]$ itself:

$$[S_1] = \int [S_1]' d[S_1]_0 = cmc \frac{A}{2} \left(s_0 - e^{-\frac{(s_0-1)^2}{2r^2}} \sqrt{\frac{2}{\pi}} r - (s_0 - 1) \operatorname{erf} \left(\frac{s_0 - 1}{\sqrt{2}r} \right) \right) + C \quad (12)$$

Now we choose the integration constant C so that $[S_1]$ is zero at $s_0=0$:

$$[S_1](0) = 0 \Rightarrow C = cmc \frac{A}{2} \left(e^{-\frac{1}{2r^2}} \sqrt{\frac{2}{\pi}} r + \operatorname{erf} \left(\frac{1}{\sqrt{2}r} \right) \right) \quad (13)$$

As last step we select the normalization constant A so that $\lim_{s_0 \rightarrow \infty} [S_1] = cmc$:

$$A = \frac{2}{1 + \sqrt{\frac{2}{\pi}} r e^{-\frac{1}{2r^2}} + \operatorname{erf} \left(\frac{1}{\sqrt{2}r} \right)} \quad (14)$$

After some rearrangement we finally get the correctly normalized model (eq (15)) for the monomer concentration $[S_1]$ with the properties we were looking for.

$$[S_1] = cmc \left[1 - \frac{A}{2} \left(\sqrt{\frac{2}{\pi}} r e^{-\frac{(s_0-1)^2}{2r^2}} + (s_0 - 1) \left(\operatorname{erf} \left(\frac{s_0 - 1}{\sqrt{2}r} \right) - 1 \right) \right) \right] \quad (15)$$

As long as the width r is not too big (see below) the monomer concentration $[S_1]$ is linear at low concentrations with an initial slope $[S_1]'$ of unity. The straight line $[S_1] = s_0$ at low s_0 always intersects with the line $[S_1]=cmc$ at the cmc ($s_0 = 1$) itself.

For small values of r the amplitude A of eq (14) is approximately $A \approx 1$. Although this is an excellent approximation for values of r below 0.5 it leads to strong deviations in $[S_1]$ for higher values of r and we strongly recommend to use the full eq (14).

Figure 1 shows plots of the correctly normalized functions $[S_1]$, $[S_1]'$ and $[S_1]''$, as given by eqs (15), (10), and (7), respectively, for different values of r and $cmc = 1$. The model function for the monomeric surfactant concentration has the expected properties. It also fulfills the criteria for the cmc mentioned above: the value of the cmc coincides with the concentration of maximum curvature [15] and the limiting straight lines intersect exactly at the cmc [28, 29]. A change in the relative transition width r does not affect the position of the cmc or the limiting slopes of $[S_1]$.

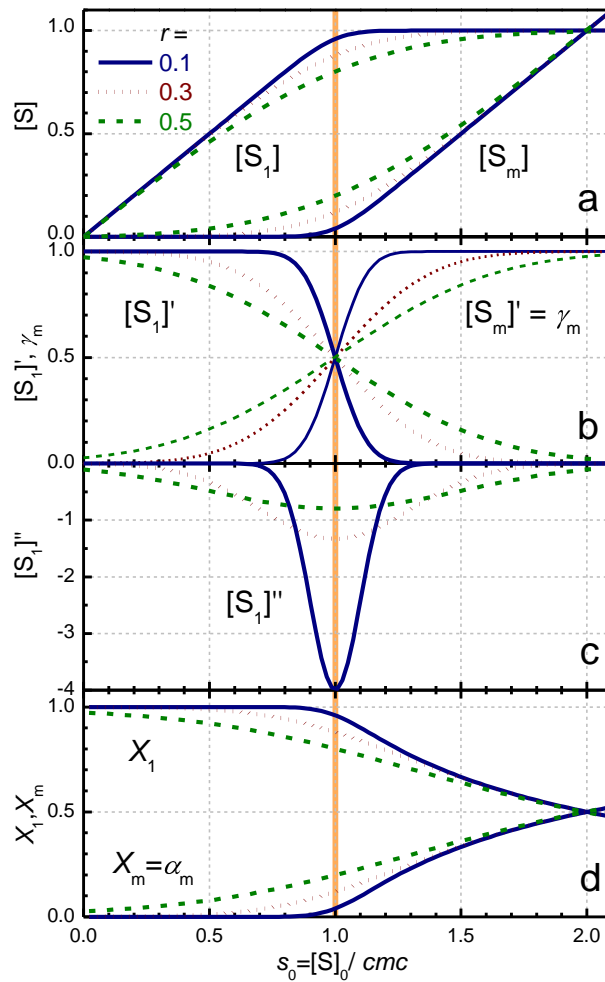


Figure 1: Different representations of the model for the concentration of monomeric surfactant $[S_1]$ as function of relative total surfactant concentration $s_0 = [S]_0 / cmc$ (eq (15)) with $cmc = 1$ and three values of the relative transition width r (solid: $r = 0.1$, dot: $r = 0.3$, dash: $r = 0.5$). (a) $[S_1]$ and $[S_m]$. (b) First derivative $d[S_1]/d[S]_0$ (eq (10)) and (differential) degree of micellization $\gamma_m = d[S_m] / d[S]_0$ (eq (16)). (c) Second derivative $d^2[S_1]/d[S]_0^2$ (eq (7)). (d) Molar fractions X_1 and X_m and degree of micellization α_m

(eq (17)). The vertical thick line indicates the *cmc*.

It should be kept in mind that the concentration model given by equations (15), (5) and (6) is based on two assumptions, which, although commonly accepted, should be evaluated in each case. First, we assume that the concentration of monomeric surfactant is constant above the *cmc*, $[S_1] = cmc$ (eqs (4) and (11)). It is known that $[S_1]$ decreases slowly at high surfactant concentration and several authors give empirical mathematical forms for some well-studied surfactants.[17, 30] Second, we assume in eq. (6) a constant aggregation number n both around the *cmc* and at high concentrations $[S]_0$. Around the *cmc* this assumption is supported by thermodynamic descriptions of the micellization process, which show that amphiphiles can only decrease their free energy significantly by forming large aggregates [29]. Small aggregates are not stable. Simulations [31] and thermodynamic models [7] seem to be in line with this assumption. Small deviations from this ideal behavior around the *cmc* would affect mainly the value of the width r . On the other hand, it is well known that the aggregation number is not constant at higher concentrations $[S]_0$. For ionic surfactants such as SDS or DTAB n increases slowly with $[S]_0$ due to the influence of the increasing concentration of counterions in solution [30, 32, 33]. Models for the dependence of n on $[S]_0$ can of course be introduced in equation (6). These approximations have different impact depending on the derived property as discussed below.

Care has to be taken with too high values of the relative transition width r . In a surfactant solution with a well-defined *cmc* no micelles are present at very dilute solutions so that the initial slope of $[S_1]$ in eq (15) should be unity (eq (4)). However, the higher the width r , the broader the transition region around the *cmc* (Figure 1). For relative widths r above approximately 0.5 the surfactant concentrations $[S_1]$ and $[S_m]$ show no initial linear region anymore and a significant fraction of micellized surfactant $[S_m]$ is predicted even in very dilute solutions. As we see in the following such high values of r correspond to surfactant mixtures or very weakly associating molecules which cannot be described by a single *cmc*.

The position of the *cmc* as defined by eq (15) coincides with the inflection point of the (differential)

degree of micellization $\gamma_m(cmc)= 0.5$ [16]:

$$\gamma_m = \frac{d[S_m]}{d[S]_0} = 1 - \frac{d[S_1]}{d[S]_0} \quad (16)$$

The value of the (fractional) degree of micellization α_m [34, 35] or molar fraction of micellized surfactant X_m at the *cmc* is given by

$$\alpha_m = X_m = \frac{n \cdot [M]}{[S]_0} = \frac{[S_m]}{[S]_0} \quad (17)$$

$$\alpha_m(cmc) = \left(\frac{[S_m]}{[S]_0} \right)_{cmc} = \frac{\sqrt{\frac{2}{\pi}} r}{1 + \sqrt{\frac{2}{\pi}} r e^{-\frac{1}{2r^2}} + \operatorname{erf} \frac{1}{\sqrt{2} r}} \approx \frac{r}{\sqrt{2\pi}} \approx 0.4 \times r \quad (18)$$

For a typical value of $r = 0.05$ to 0.1 the degree of micellization $\alpha_m(cmc)$ is 0.02 to 0.04 , which means that at the *cmc* only 2% to 4% of the surfactants form micelles (See Figure 1, d). This compares very well with the value of $\varepsilon = \alpha_m(cmc) = 0.02$ used in the mass action model for the definition of the *cmc* [17, 36]. This approximately linear relation between $\alpha_m(cmc)$ and r is valid up to quite high values of r , with an error of less than 0.5% at $r = 0.5$.

As next step we use the concentration model to derive specific equations for different physical properties: conductivity, surface tension, NMR shifts and self-diffusion coefficients. It is not our aim to give an exhaustive or critical review of each of the properties, but we mainly illustrate the use and validity of the model.

Electrical conductivity of ionic surfactant solutions

The conductivity (specific conductance) of a solution of an anionic surfactant of concentration $[S]_0$ with monomer concentration $[S_1]$ and micelle concentration $[M]$ is given by [37]

$$\begin{aligned} \kappa &= \underbrace{(\lambda_{C^{+}} + \lambda_{S^{-}})}_a [S_1] + \underbrace{(\lambda_{M^{z-}} + z\lambda_{C^{+}})}_{b'} [M] + \kappa_s \\ &= a[S_1] + b'[M] + \kappa_s \end{aligned} \quad (19)$$

with the molar conductivities of monomeric surfactant anions $\lambda_{S^{-}}$, of counter-cations $\lambda_{C^{+}}$, and of micelles $\lambda_{M^{z-}}$. Each micelle of net charge $z \cdot e$ and aggregation number n incorporates $(n - z)$ counterions,

and leaves z counterions free in solution. κ_s is the residual conductivity of the solvent without surfactant. With $[M] = [S_m] / n$ and $b = b'/n$ we get

$$\kappa = a[S_1] + b'[S_m]/n + \kappa_s = a[S_1] + b[S_m] + \kappa_s \quad (20)$$

The parameters a , b and κ_s can be determined by fits of eq (20) to conductivity data using eqs (15) and (5) in order to calculate the concentrations $[S_1]$ and $[S_m]$ as functions of total surfactant concentration $[S]_0$.

The parameters a and b have units of molar conductivity and are the slopes of the limiting straight lines κ_1 and κ_2 observed at low and high concentration of surfactant, respectively. κ_1 and κ_2 are given by:

$$\begin{aligned} \kappa_1 &= a[S]_0 + \kappa_s \\ \kappa_2 &= a \cdot cmc + b \cdot ([S]_0 - cmc) + \kappa_s \end{aligned} \quad (21)$$

The degree of ionization $\alpha = n - z / n$ of the micelle can be calculated according to Evans [38-41] as

$$\alpha = -\frac{\lambda_{C^+} - \sqrt{4bn^{2/3}(a - \lambda_{C^+}) + \lambda_{C^+}^2}}{2n^{2/3}(a - \lambda_{C^+})} \quad (22)$$

The molar conductivity (equivalent conductance) Λ_m is given by:

$$\Lambda_m = (\kappa - \kappa_s)/[S]_0 = a[S_1]/[S]_0 + b[S_m]/[S]_0 \quad (23)$$

The molar conductivities of monomeric surfactant anions λ_{S^-} , and of micelles $\lambda_{M^{z-}}$ are given by:

$$\begin{aligned} \lambda_{S^-} &= a - \lambda_{C^+} \\ \lambda_{M^{z-}} &= n(1 - \alpha)\lambda_{C^+} - b \end{aligned} \quad (24)$$

The equations for cationic surfactants are analogous.

A concentration dependent aggregation number n affects the contribution of the micelles to the overall conductivity in two opposite ways: an increase of n reduces the concentration of micelles $[M]$ but at the same time increases the molar conductivity of each of the micelles. In the case of SDS a dependence of the conductivity of micelles $\lambda_{M^{z-}} \cdot [M]$ on $[S]_0$ of the order of $[S]_0^{1/6}$ is predicted [17, 24, 33].

Surface Tension

The surface tension of a surfactant solution can be approximately described by the Szyszkowski equation:

$$\gamma = \gamma_0 - a \ln(1 + K_{ad} \cdot [S_1]) \quad (25)$$

with the adsorption equilibrium constant K_{ad} , the surface tension of the solvent γ_0 , and the constant $a = R \cdot T / \omega$, ω being the cross sectional area of the surfactant molecule at the surface per mol [42-44]. In contrast to monomers, micelles are not surface active. Therefore we use $[S_1]$ as concentration which defines the surface tension. Surface tension is not affected by variations in the aggregation number n .

Chemical Shift in NMR Experiments

Due to the fast exchange [4, 45] of a surfactant molecule between the aqueous and the micellar pseudo-phase, the chemical shift δ_{obs} of the resonance peak of the surfactant observed in NMR spectra can be expressed as weighted mean of the chemical shifts δ_1 and δ_m of monomeric and micellized surfactant, respectively: [46]

$$\delta_{obs} = \delta_1 \cdot \frac{[S_1]}{[S]_0} + \delta_m \cdot \frac{[S_m]}{[S]_0} = (\delta_1 - \delta_m) \cdot \frac{[S_1]}{[S]_0} + \delta_m \quad (26)$$

Since each of the surfactants in a micelle contributes to the signal the observed shift is weighted by the concentration of micellized surfactants $[S_m]$ and not by $[M]$ and is therefore also not affected by variations in n . Shifts of several nuclei can of course be fitted globally.

Diffusion Coefficient

Self-Diffusion coefficients as measured by NMR or Taylor dispersion are average diffusion coefficients, weighted with the concentration of monomeric and micellized surfactants: [47]

$$D_{obs} = D_1 \cdot \frac{[S_1]}{[S]_0} + D_m \cdot \frac{[S_m]}{[S]_0} \quad (27)$$

The weighting is specific to each technique and care has to be taken to apply a correct expression. Light scattering measures mutual diffusion coefficients [48], whereas PGSE-NMR yields self-diffusion coefficients [47].

Eqs (26) and (27) are of the same type, where the observed property ϕ_{obs} is the sum of the individual properties of monomeric ϕ_l and micellized ϕ_m surfactants weighted with their molar fractions X_l and X_m . As for the chemical shifts, these self-diffusion coefficients depend on the concentration of each of the micellized surfactants $[S_m]$. Depending on the technique variations in the aggregation number n can affect the diffusion coefficient D_m .

Results and Discussion

The concentration model (eqs (15) and (5)) and the functions of the derived properties are used to analyze experimental data of several surfactant systems studied with different techniques. First, conductivity, surface tension, NMR shift, and diffusion data of the well-studied anionic surfactant SDS are studied, then conductivity data of other surfactants with lower *cmc* values and polydisperse surfactants which are notoriously difficult to treat by graphical extrapolation procedures.

SDS, Conductivity: Figure 2 shows the conductivity of the anionic surfactant sodium dodecyl sulfate (SDS) in pure water at 25°C. SDS is a well-studied surfactant with a well-defined *cmc* of 8.1- 8.2 mM and an aggregation number of 62-64 at 25°C [10, 13, 28]. The fit of model (20) to the data, with $[S_l]$ and $[S_m]$ given by eqs (15) and (5), respectively, is excellent (see Figure 2). The model reproduces the data remarkably well, with randomly distributed residuals, only limited by the digital resolution of the conductivity meter used for the measurement. Even around the *cmc* the deviation is less than 0.2%, of the order of the reproducibility of the instrument.

The *cmc* = 8.099 mM is determined with high precision and coincides well with reference data (Table 1). The relative width $r = 0.112$ corresponds to a width of the transition region $\sigma = 0.9$ mM (see eq (7)). The interval $cmc \pm 2\sigma$ is shown as inset in Figure 2. The slopes $a = 66.74 \pm 0.03$ S cm² mol⁻¹ and $b = 26.43 \pm 0.01$ S cm² mol⁻¹, the derived micelle ionization degree $\alpha = 0.236$ (eq (22), $\lambda_{c^+}(\text{Na}^+) = 50.08$ S cm² mol⁻¹) [49] and the slope ratio $b/a = 0.396$ coincide well with published data [41]. From this data

the molar conductivities of monomeric surfactant anions $\lambda_{S^-} = 16.66 \pm 0.03 \text{ S cm}^2 \text{ mol}^{-1}$, and of micelles $\lambda_{M^{2-}} = 732 \pm 24 \text{ S cm}^2 \text{ mol}^{-1}$ are obtained.

The straight lines κ_1 and κ_2 calculated with the parameters of the fit and eq (21) intersect exactly at the *cmc*, which is an intrinsic property of the model (20).

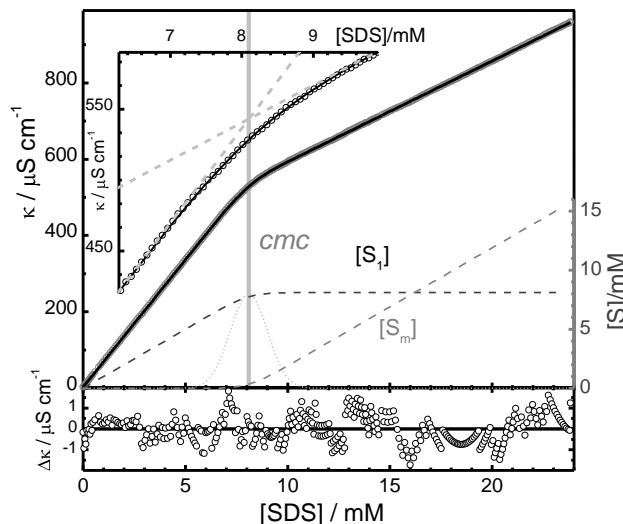


Figure 2: Conductivity κ of SDS in aqueous solution at 298K. Circles: experimental data (the 330 data points appear as thick line). Black solid line: fit of model (20) to the data. Dashed grey lines: concentrations $[S_1]$ and $[S_m]$ from eqs (15) and (5). Dotted grey line: second derivative of $[S_1]$ (eq (7)). Vertical grey line: *cmc* as given by the fit. Insert: Zoom of the interval $[S]_0 = [cmc - 2\sigma, cmc + 2\sigma] = [6.3 \text{ mM}, 9.9\text{mM}]$. Grey lines: limiting straight lines κ_1 and κ_2 as given by eq (21). Lower panel: residuals of the fit.

It is well known that different ways to plot the same experimental data can give significantly different values of the *cmc* determined by graphical extrapolating procedures [13]. A typical example is the comparison of plots of conductivity κ to that of molar conductivity (equivalent conductance) Λ_m represented against the total surfactant concentration (or against its square root). The limiting straight lines which can be drawn through the data within a sufficiently small concentration interval around the *cmc*, do not generally intersect at the same concentration in the two types of plots. Figure SII in the Supporting Information shows the same data as in Figure 2, converted to molar conductivity

$\Lambda_m = (\kappa - \kappa_s)/[S]_0$. Within a smaller concentration range around the *cmc* (interval indicated in the figure as dashed rectangle) straight lines may be drawn through the data with intersections at concentrations of 7.71mM in the plot of Λ_m vs. $[S]_0^{1/2}$ and 7.64mM in the plot of Λ_m vs. $[S]_0$. These concentrations do not coincide and both are significantly smaller than the *cmc* = 8.099 mM determined from the conductivity in Figure 2. This problem does not arise if eq (23) (with eq (15) for $[S_1]$) is fitted to the molar conductivity, which gives of course the same parameter values as in the case of the conductivity, with exactly the same *cmc*. The parameters of model (15) are independent of whether we analyze the same data as κ or as Λ_m plotted against $[S]_0$ or $[S]_0^{1/2}$ (see Table 1). The only differences arise due to slightly different weighting of the experimental errors in the fits, as can be seen in the residuals of the two types of plots (Figures 2 and S11).

Thus the fit of model (15) allows one to determine consistent values of the parameters between the different plots.

Table 1: Values of the *cmc*, *r*, micelle ionization ratio α (eq (22)), and slope ratio *b/a* for different surfactants and techniques obtained from the fits of eqs (19) - (27) together with model eq (15) for $[S_1]$ and (5) for $[S_m]$ to the data shown in the corresponding figures. The uncertainties are standard deviations from the fit.

Surfactant	Technique	Ref ^d	Figure	<i>cmc</i> / mM	<i>r</i>	α	<i>b/a</i>	<i>T/K</i>
SDS	Conductivity		2	8.099±0.005	0.112±0.001	0.236	0.396	298
SDS	Molar conductivity		S11	8.099±0.004	0.112±0.001	0.236	0.396	298
SDS	Surface Tension	[50]	3	7.7±0.1 7.6±0.2	0.03±0.04 0.1 fixed	-	-	293
SDS ^b	NMR, Diffusion	[51]	4	7.35±0.09	0.10±0.03	-	-	298
DTAB	Conductivity		5a	14.5±0.2	0.16±0.04	0.18	0.24	298
CTAB ^c	Conductivity		5b	0.88±0.07	0.1±0.2	-	0.75	293
LAS	Conductivity		5c	1.64±0.02	0.48±0.02	0.28- 0.35	0.53	293

^aSource for experimental data. ^bin D₂O, ^cin phosphate solution, ionic strength = 0.01M.

SDS, Surface Tension: Figure 3 shows surface tension data obtained with SDS solutions at 20°C by

Watanabe et al. [50] The data are plotted against SDS concentration $[S]_0$ both with a linear scale (lower axis) and with logarithmic scale (upper axis). It is not our aim to discuss neither the technique nor the results of the authors, but merely to illustrate the application of our concentration model to this type of data. The authors determine the *cmc* as the point of intersection of two straight lines in a plot of surface tension γ versus SDS concentration to be about $2200 \text{ mg kg}^{-1} = 7.6 \text{ mM}$. Figure 3 shows that no linear behavior of the data below the *cmc* is found in such a plot and drawing a straight line in this interval is quite arbitrary. The analysis with the Szyszkowski eq (25) together with model (15) for the surfactant monomer concentration is independent of the type of plot and yields an excellent fit with a value of the *cmc* of $7.7 \pm 0.1 \text{ mM}$, a relative transition width $r = 0.03 \pm 0.04$, and the other fit parameters: $a = 28 \pm 2 \text{ mN m}^{-1}$, $K_{ad} = 0.3 \text{ mM}^{-1}$ and $\gamma_0 = 68.3 \pm 0.4 \text{ mN m}^{-1}$ (Table 1). The width r is not well defined, which is mainly due to the small number of experimental points. Furthermore, it is also well known that already very small concentrations of surface active impurities affect the transition region around the *cmc* [27]. However, the value of r has nearly no influence on that of the *cmc*, and the fit with fixed value $r = 0.1$ gives the same *cmc*-value with higher uncertainty due to a slightly worse fit (Table 1). This value of the *cmc* coincides well with that determined from extrapolation in the logarithmic plot in Figure 3, but is somewhat lower than that of the conductivity data, which is probably due to the different measurement temperature and the mentioned sensitivity to impurities.

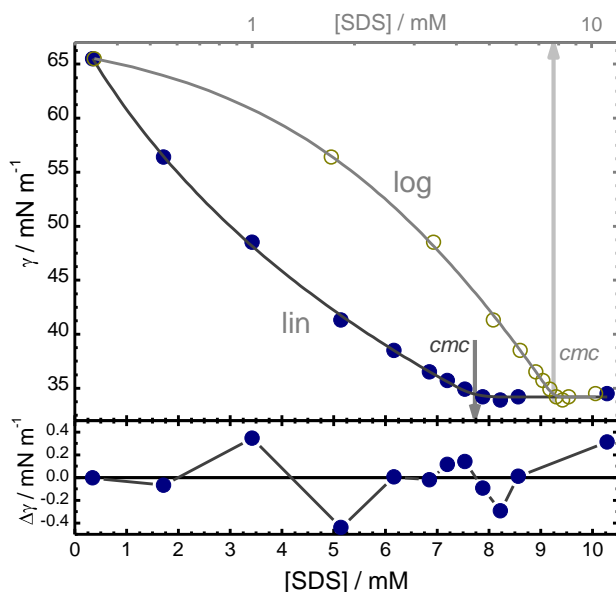


Figure 3: Surface tension γ of SDS in water at 293K from Watanabe et al. converted from mg kg^{-1} to $10^{-3} \text{ mol dm}^{-3}$ (mM) [50]. Linear plot (lower axis) of experimental data (filled circles) and fit of eq (25) to the data (solid lines). Lin-Log plot (upper axis) of the same experimental data (open circles) and of the fit data (grey line). Vertical grey arrows: *cmc* as given by the fit. Lower panel: residuals of the fit in the linear plot.

SDS, NMR: Data of chemical shifts δ_{obs} of protons H1 and H5 and self-diffusion coefficients D_{obs} of SDS in D2O from NMR experiments published by Cui et al. are shown in Figure 4 [51]. The authors use plots of δ_{obs} and D_{obs} against reciprocal surfactant concentration $[S]_0^{-1}$ and determine the *cmc* from straight lines drawn through some of the experimental points. We performed the fits of eqs (26) and (27) to the data which are excellent in each case, also in the region around the *cmc*. We find no evidence for the formation of “premicelles” as the authors propose.

The use of the eqs (26) and (27) in standard nonlinear optimization routines makes it now possible to perform a *global analysis* of all three data series together in one fit, sharing the *cmc* and *r* as common fit parameters. Global fitting is preferred over single fits as it reduces the number of fit parameters and the correlations between them and improves the statistics of the fit [52]. The global fit of $\delta_{\text{obs}}(\text{H1})$, $\delta_{\text{obs}}(\text{H5})$ and D_{obs} is excellent, as shown in Figure 4, with shared values of *cmc* and *r* given in Table 1 and

$D_1=5.04\pm 0.03 \cdot 10^{-10} \text{ m}^2\text{s}^{-1}$, $D_m=0.28\pm 0.06 \cdot 10^{-10} \text{ m}^2\text{s}^{-1}$, $\delta_1(\text{H1}) = 0.92\pm 0.02 \text{ ppm}$, $\delta_m(\text{H1}) = 0.97\pm 0.04 \text{ ppm}$, $\delta_1(\text{H5}) = 4.12\pm 0.02 \text{ ppm}$, $\delta_m(\text{H5}) = 4.09\pm 0.04 \text{ ppm}$. (The analysis software used for the global fit does not allow the use of different fitting functions is the same fit. However, we take advantage of the fact that both equations (26) and (27) have the same mathematical form.)

This example illustrates the great potential of the concentration model for the quantitative analysis of NMR data, and even for global analysis, which are, in our opinion, very superior to the graphical extrapolation methods typically applied.

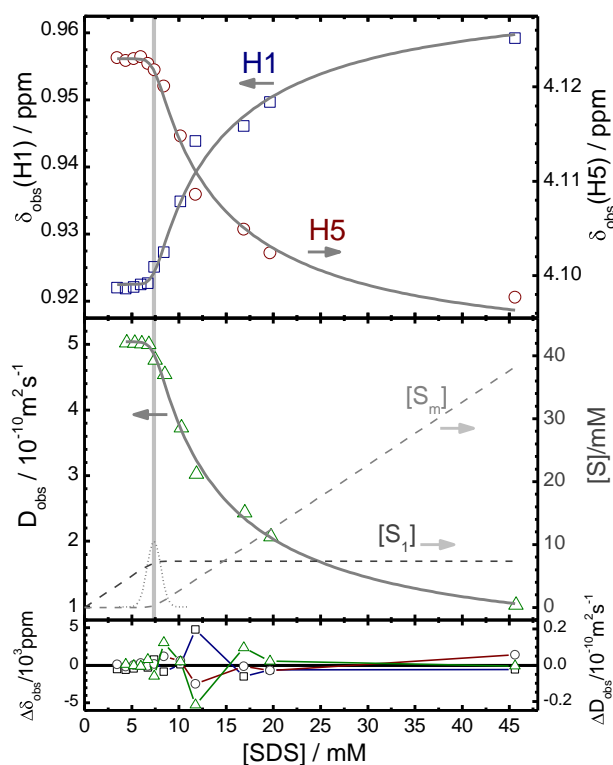


Figure 4: ^1H NMR chemical shifts δ_{obs} (upper panel) of protons H1 (quadrats) and H5 (circles) and NMR self-diffusion coefficients D_{obs} (middle panel, triangles) of SDS in D_2O at 298K published by Cui et al. [51] Grey solid lines: global fit of eqs (26) and (27) to the data. Vertical line: *cmc* as given by the fit. Dashed grey lines: simulated concentrations $[S_1]$ and $[S_m]$. Dotted grey line: second derivative of $[S_1]$. Lower panel: residuals of the fits.

DTAB, Conductivity: Figure 5a shows the conductivity of DTAB in aqueous solution as function of surfactant concentration at 298K. The fit with eqs (20) and (15) gives a *cmc* of $14.5\pm 0.2 \text{ mM}$ and a

width of $r = 0.16 \pm 0.04$ with slopes $a = 103 \pm 1 \text{ S cm}^2 \text{ mol}^{-1}$, $b = 24.4 \pm 0.4 \text{ S cm}^2 \text{ mol}^{-1}$ (Table 1). The cmc coincides well with reported values of 14.5 mM-15.3mM [13, 53, 54]. In spite of the low number of data points, both cmc and r are still reliably determined. The relative transition width r is similar to that obtained for SDS (Table 1). From the slopes and eq (22) the slope ratio $b/a=0.24$ and a micelle ionization degree $\alpha = 0.18 \pm 0.01$ are obtained (with $\lambda(\text{Br}^-) = 78.1 \text{ S cm}^2 \text{ mol}^{-1}$ [49] and $n = 50$ [4, 54]). The value of α is lower than reported values of 0.21[11, 54] or 0.26 ± 0.01 [33]. The data yield the molar conductivities of monomeric surfactant cations $\lambda_{\text{S}^+} = 25 \pm 1 \text{ S cm}^2 \text{ mol}^{-1}$, and of micelles $\lambda_{\text{M}^{\text{st}}} = (1.76 \pm 0.02) 10^3 \text{ S cm}^2 \text{ mol}^{-1}$.

This example shows that, even in the case of a low number of data points, the model fits conductivity data satisfactorily and yields precise values for several properties of the surfactant.

CTAB, Conductivity: The conductivity of CTAB in phosphate solution (ionic strength = 0.01M) as function of $[\text{S}]_0$ serves here as an example of a system which is notoriously difficult to analyze graphically. The plot of κ against $[\text{S}]_0$ (Figure 5b) shows only a very small change in the slope around the cmc which makes it difficult to determine the point of intersection of the limiting lines graphically. On the contrary, eq (20) for κ with eqs (15) and (5) for $[\text{S}_1]$ and $[\text{S}_m]$, respectively, fit fast and reliably to the data and give a relatively precise value of the $cmc = 0.88 \pm 0.07 \text{ mM}$. This value is lower than the reported value [16, 55] of 0.92 mM, due to the higher ionic strength of the solution.

The low number of experimental points and the small change in the slopes increase the uncertainty in the value of the relative transition width $r = 0.1 \pm 0.2$, but its mean value is reasonable and similar to the values determined before. The fit yields slopes of $a = 33.2 \pm 0.9 \text{ S cm}^2 \text{ mol}^{-1}$, and $b = 25.0 \pm 0.4 \text{ S cm}^2 \text{ mol}^{-1}$, and $\kappa_s = 1417.1 \pm 0.4 \mu\text{S cm}^{-1}$ with a ratio $b/a = 0.75$ (Table 1).

Due to the additional salt in solution both the aggregation number and the molar conductivity of the counter-ion is changed with respect to the known values in pure water.

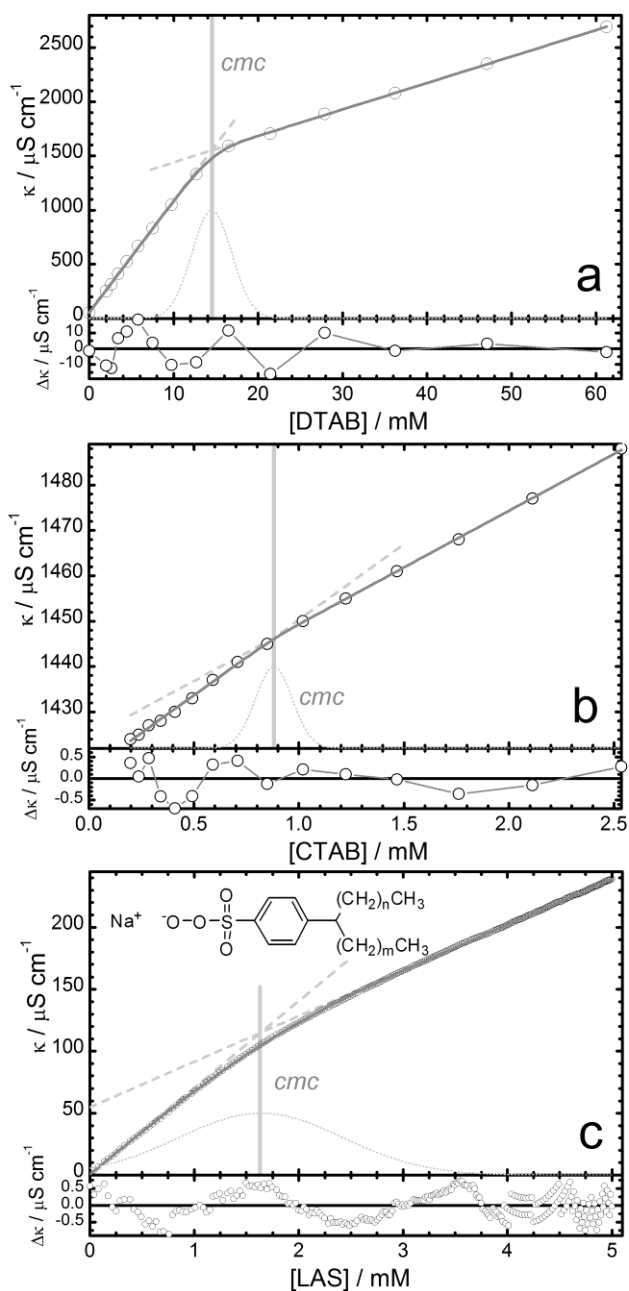


Figure 5: Conductivity κ of DTAB (a), CTAB (b), and LAS (c) in aqueous solution at 298K (CTAB in phosphate solution, ionic strength = 0.01M). Open circles: experimental data, grey solid line: fit of models (20) and (15) to the data. Dotted grey line: second derivative of $[S_1]$ (eq (7)) with a width given by the fit. Vertical grey line: cmc as given by the fit. Dashed grey lines: limiting straight lines κ_1 and κ_2 as given by eq (21). Lower panels: residuals of the fits.

LAS, Conductivity: LAS (Sodium linear alkylbenzene sulfonate) is an important commercial anionic surfactant which consist in a complex mixture of homologues of different alkyl chain lengths (C10 to

C13 or C14) and phenyl positional isomers with polydisperse chain lengths n and m , with a mean value of 11.6 (see structure in Figure 5c) [56]. Again this is an example with a small change in the slopes of the conductivity-concentration plot (Figure 5c). Additionally, each isomer with different chain lengths n and m has a slightly different cmc which results in a wider transition region in the conductivity plot. The fit of eq (20) with $[S_1]$ and $[S_m]$ given by eqs (15) and (5), respectively, converges reliably with $cmc = 1.64 \pm 0.02$ mM and a width $r = 0.48 \pm 0.02$, which is high, as expected for this polydisperse surfactant. The cmc is similar to that determined by surface tension (1.8 mM) [57]. The slopes are $a = 69.9 \pm 0.5$ S cm² mol⁻¹ and $b = 36.86 \pm 0.06$ S cm² mol⁻¹ with a ratio $b/a = 0.53$ (Table 1).

The micelle ionization degree α (eq (22)) depends weakly on the aggregation number n . For LAS values of n between 27 and 65 were reported.. These values lead to ionization degrees α between 0.28 and 0.35 (with $\lambda_{c^+}(\text{Na}^+) = 50.08$ S cm² mol⁻¹) [49].

In spite of the small change in the slopes and the wide transition region reliable values for the cmc and the slopes are obtained in a single fit. However, in this case a small but significant oscillation of the residuals is observed (lower panel in Figure 5c), in contrast to SDS (Figure 2). This may indicate that this surfactant mixture is not adequately described by a single cmc with high r but should rather be fitted with a cmc distribution.

Conclusion

The empirical concentration model presented here constitutes a useful tool for the quantitative analysis of experimental data obtained with different techniques from surfactant solutions. The model establishes an objective definition of the cmc and makes it possible to obtain precise and well defined values of derived physical parameters such as molar conductivities, micelle ionization degrees, surface adsorption equilibrium constants, self-diffusion coefficients, etc. The description of different properties with a common concentration model eliminates subjective graphical procedures, reduces methodological differences and allows one thus to compare directly the results of several techniques or even to analyze them simultaneously in a single global fit. The concentration model can also serve as a robust and fast

method to determine the *cmc* in automated high throughput applications [58-60].

The monodisperse surfactants with well-defined *cmc*, SDS, DTAB or CTAB, are very well described with the models based on eq (15) with relative transition widths r around 0.1 and values of the *cmc* which coincide well with published data. A higher value of the transition width r is obtained for LAS, which is a complex mixture of homologues and isomers, each with different *cmc* values.

The values obtained for the *cmc* of SDS from the different experimental datasets (Table 1) show significant differences, in spite of the use of the same concentration model in the analysis. Apart from the influence of temperature, impurities and solvents, the differences in the *cmc* values also reflect the fact that the data were measured with different techniques in various laboratories and with strongly varying accuracy. The value obtained from conductivity in our lab with an estimated accuracy of about 0.5%, coincides very well with reported values [13, 28]. Surface tension data is known to be strongly sensitive to even small surface-active impurities, and thus the coincidence is quite satisfactory [13]. The chemical shift and diffusion data obtained from NMR give clearly a too low *cmc*-value, a fact that the authors already mentioned, but did not justify [51]. Nevertheless, the data serve the only purpose of demonstrating the application of the concentration model, and a critical evaluation of these values is beyond the scope of this contribution.

The concentration model also allows us to plot in a quantitative manner the concentration dependence of several physical properties of the same micelle-forming amphiphile, according to the schematic representation published by Preston [61], and by Lindman and Wennerström [12]; and later reproduced in many textbooks [27, 37]. Figure 6 shows such a plot with the properties studied in this contribution for an aqueous SDS solution: conductivity, molar conductivity, surface tension, NMR chemical shift, and NMR self-diffusion coefficient. In order to obtain a useful didactic representation, we plotted all properties with the parameters obtained from the fits, except for the value of the *cmc*, which is set to 8 mM in all cases. We also added the concentrations $[S_1]$ and $[S_m]$ and the second derivative (curvature) $[S_1]''$. The simple implementation of the concentration model and the possibility to compare easily

derived properties will hopefully also be of didactic use. It is instructive to see, that the effect of micellization affects the properties already well before the *cmc*, and that the process of micellization is not described by a sharply defined point, as often represented in textbooks, but rather by a gradual change in the degree of micellization.

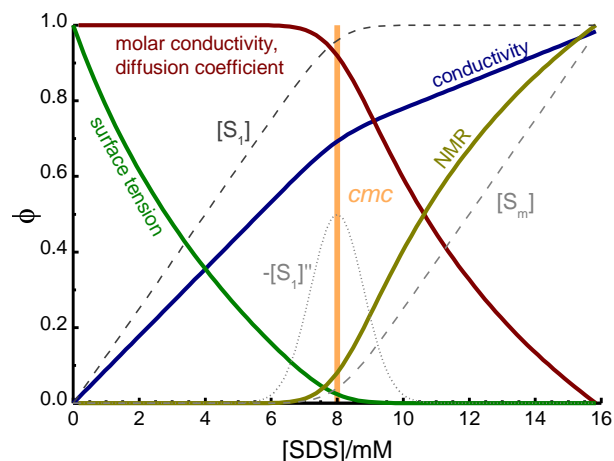


Figure 6: Normalized physical-chemical properties of an aqueous SDS solution as function of total surfactant concentration $[S]_0$ with the parameters determined from the fits to the experimental data presented above using the concentration model of eq (15). Solid curves: Conductivity κ (eq (20)), molar conductivity Λ_m (eq (23)), surface tension γ (eq (25)), ^1H NMR chemical shift δ (eq (26)) and NMR self-diffusion coefficient D (eq (27)). Dashed curves: concentration of monomeric surfactant $[S_1]$ (eq (15)) and concentration of micellized surfactant $[S_m]$ (eq (5)) Dotted curve: second derivative of $[S_1]$ (eq (7)). The curves of Λ_m , D , and $\delta(\text{H5})$ overlap. The vertical solid line indicates the *cmc*. ($cmc = 8\text{mM}$, $r = 0.1$, all other parameters as given in the corresponding figure captions above and in Table 1)

A natural consequence of the gradual change in micellization is the presence of micellized surfactant already below the point taken as *cmc*. The concentration $[S_m]$, its fraction $[S_m]/[S]_0$, and the degree of micellization all are expected to change already below the *cmc*, as can be seen in Figure 1. The models based on eq (15) together with the assumption of constant aggregation number n describe extremely well the conductivity data of SDS measured with high precision (Figure 2), but also the surface tension, NMR chemical shifts, and the self-diffusion data. The gradual formation of low concentrations of

micelles with full size n explains perfectly the variation observed in the experimental data around and below the *cmc*. Therefore, at least in the systems studied here, we find no evidence for the formation of surfactant aggregates such as the so called “premicelles”, with different properties to the proper micelles.

ACKNOWLEDGMENTS: L.P. thanks the Gil Dávila Foundation for a scholarship. M.N. and W.A. thank the Ministerio de Ciencia e Innovación and the Xunta de Galicia for financial support (CTQ2010-21369, INCITE09262304PR, INCITE09E2R209064ES, IN845B-2010/094).

Supplementary data: Additional figures and fitting functions for Origin data analysis software.

References

- [1] K. Holmberg, Handbook of Applied Surface & Colloid Chemistry, John Wiley & Sons Inc, 2001.
- [2] T.F. Tadros, Applied Surfactants: Principles and Applications, VCH Verlagsgesellschaft, 2005.
- [3] J.N. Israelachvili, Intermolecular and Surface Forces, Academic Press, New York, 2010.
- [4] R. Zana, Dynamics of Surfactant Self-Assemblies: Micelles, Microemulsions, Vesicles, and Lyotropic Phases, Taylor & Francis/CRC Press, Boca Raton, 2005.
- [5] D. Blankschtein, A. Shiloach, N. Zoeller, Current opinion in colloid & interface science. 2 (1997) 294.
- [6] B.C. Stephenson, K. Beers, D. Blankschtein, Langmuir. 22 (2006) 1500.
- [7] R. Hadgiivanova, H. Diamant, J Phys Chem B. 111 (2007) 8854.
- [8] M. Sammalkorpi, S. Sanders, A. Panagiotopoulos, M. Karttunen, M. Haataja, J. Phys. Chem. B. (2011) .
- [9] A. Gezae Daful, V. Baulin, J. Avalos, A. Mackie, J. Phys. Chem. B. 115 (2011) 3434.
- [10] N.J. Turro, A. Yekta, J. Am. Chem. Soc. 100 (1978) 5951.
- [11] S. Freire, J. Bordello, D. Granadero, W. Al Soufi, M. Novo, Photochem. Photobiol. Sci. 9 (2010) 687.
- [12] B. Lindman, H. Wennerstrom, Top. Curr. Chem. 87 (1980) 1.
- [13] P. Mukerjee, K.J. Mysels, Critical Micelle Concentrations of Aqueous Surfactant Systems, NIST National Institute of Standards and Technology, Washington D.C. USA, 1971.
- [14] A. Patist, in Handbook of Applied Surface and Colloid Chemistry, K. Holmberg (Ed.), John Wiley & Sons:

New York, 2001, p. 239.

- [15] J. Phillips, *Transactions of the Faraday Society*. 51 (1955) 561.
- [16] I. García-Mateos, M. Mercedes Velázquez, L.J. Rodríguez, *Langmuir*. 6 (1990) 1078.
- [17] P. Shanks, E. Franses, *J. Phys. Chem.* 96 (1992) 1794.
- [18] M. Pérez-Rodríguez, G. Prieto, C. Rega, L.M. Varela, F. Sarmiento, V. Mosquera, *Langmuir*. 14 (1998) 4422.
- [19] P. Carpena, J. Aguiar, P. Bernaola-Galván, C.C. Ruiz, *Langmuir*. 18 (2002) 6054.
- [20] K. Shinoda, E. Hutchinson, *J. Phys. Chem.* 66 (1962) 577.
- [21] R.F. Kamrath, E.I. Franses, *Industrial & Engineering Chemistry Fundamentals*. 22 (1983) 230.
- [22] M.E. Moro, L.J. Rodriguez, *Langmuir*. 7 (1991) 2017.
- [23] J.L. López Fontán, J. Costa, J. Ruso, G. Prieto, F. Sarmiento, *The European Physical Journal E: Soft Matter and Biological Physics*. 13 (2004) 133.
- [24] N. Jalsenjak, D. Tezak, *Chemistry-a European Journal*. 10 (2004) 5000.
- [25] A. Jover, F. Meijide, V. Mosquera, J. Vázquez Tato, *J. Chem. Educ.* 67 (1990) 530.
- [26] M.J. Rosen, *Surfactants and Interfacial Phenomena*, John Wiley & Sons, Inc., 2004.
- [27] I. Hamley, *Introduction to Soft Matter. Revised Edition*, Wiley Online Library, 2007.
- [28] R. Williams, J. Phillips, K. Mysels, *Trans. Faraday Soc.* 51 (1955) 728.
- [29] J.N. Israelachvili, D.J. Mitchell, B.W. Ninham, *Journal of the Chemical Society, Faraday Transactions 2: Molecular and Chemical Physics*. 72 (1976) 1525.
- [30] F.H. Quina, P.M. Nassar, J.B.S. Bonilha, B.L. Bales, *J. Phys. Chem.* 99 (1995) 17028.
- [31] S. Morisada, H. Shinto, *J. Phys. Chem. B*. 114 (2010) 6337.
- [32] V.Y. Bezzobotnov, S. Borbely, L. Cser, B. Farago, I. Gladkih, Y.M. Ostanevich, S. Vass, *J. Phys. Chem.* 92 (1988) 5738.
- [33] B.L. Bales, R. Zana, *J Phys Chem B*. 106 (2002) 1926.
- [34] A.K. Shchekin, A.P. Grinin, F.M. Kuni, A.I. Rusanov, in *Nucleation Theory and Applications*, J.W.P. Schmelzer, G. Röpke, V.B. Priezhev (Eds.), Wiley-VCH Verlag GmbH & Co. KGaA, 2005, p. 312.

- [35] O. Us' yarov, *Colloid Journal*. 66 (2004) 612.
- [36] R. Kamrath, E. Franses, *J. Phys. Chem.* 88 (1984) 1642.
- [37] R.J. Hunter, *Foundations of Colloid Science*, Oxford University Press, 2001.
- [38] H. Evans, *J.Chem.Soc.* (1956) 579.
- [39] L. Sepulveda, J. Cortes, *J. Phys. Chem.* 89 (1985) 5322.
- [40] B.L. Bales, *J. Phys. Chem. B.* 105 (2001) 6798.
- [41] M. Benrraou, B.L. Bales, R. Zana, *J. Phys. Chem. B.* 107 (2003) 13432.
- [42] B. Szyszkowski, *Z. Phys. Chem.* 64 (1908) 385.
- [43] K.J. Mysels, *Langmuir*. 2 (1986) 423.
- [44] V. Fainerman, R. Miller, *Langmuir*. 12 (1996) 6011.
- [45] M. Novo, S. Felekyan, C.A.M. Seidel, W. Al-Soufi, *J Phys Chem B.* 111 (2007) 3614.
- [46] M. Amato, E. Caponetti, D.C. Martino, L. Pedone, *J. Phys. Chem. B.* 107 (2003) 10048.
- [47] O. Annunziata, L. Costantino, G. D'Errico, L. Paduano, V. Vitagliano, *J. Colloid Interface Sci.* 216 (1999) 16.
- [48] E. Sutherland, S.M. Mercer, M. Everist, D.G. Leaist, *Journal of Chemical & Engineering Data.* 54 (2008) 272.
- [49] R.C. Weast, *CRC Handbook of Chemistry and Physics*, CRC Press, Boca Raton, Florida, 1986.
- [50] K. Watanabe, S. Niwa, Y.H. Mori, *Journal of Chemical & Engineering Data.* 50 (2005) 1672.
- [51] X. Cui, S. Mao, M. Liu, H. Yuan, Y. Du, *Langmuir*. 24 (2008) 10771.
- [52] J.M. Beechem, *Meth. Enzymol.* 210 (1992) 37.
- [53] S. Kato, H. Nomura, R. Zielinski, S. Ikeda, *J. Colloid Interface Sci.* 146 (1991) 53.
- [54] P.C. Hiemenz, R. Rajagopalan, *Principles of Colloid and Surface Chemistry*, Marcel Dekker, New York, 1997.
- [55] K. Kalyanasundaram, *Photochemistry in Microheterogeneous Systems*, Academic Press, New York, 1987.
- [56] N.M. van Os, R. Kok, T.A.B.M. Bolsman, *Tenside Surfactants Detergents.* 29 (1992) 175.

- [57] P. Goon, C. Manohar, V.V. Kumar, *J. Colloid Interface Sci.* 189 (1997) 177.
- [58] S. Paillet, B. Grassl, J. Desbrières, *Anal. Chim. Acta.* 636 (2009) 236.
- [59] C.H. Tan, Z.J. Huang, X.G. Huang, *Anal. Biochem.* 401 (2010) 144.
- [60] T. Jumpertz, B. Tschapek, N. Infed, S.H.J. Smits, R. Ernst, L. Schmitt, *Anal. Biochem.* (2010) .
- [61] W.C. Preston, *J. Phys. Chem.* 52 (1948) 84.
- [62] M. Kline, *Calculus: An Intuitive and Physical Approach*, Dover Pubns, 1998.